J. Plasma Physics (2012), *vol.* 78, *part* 2, *pp.* 175–180. © Cambridge University Press 2011
doi:10.1017/S0022377811000547

Arbitrary amplitude Langmuir solitons in a relativistic electron–positron plasma

I. J. LAZARUS[1], R. BHARUTHRAM[2], S. V. SINGH[3,4] and G. S. LAKHINA[3]

[1]Department of Physics, Durban University of Technology, Durban, South Africa
[2]University of the Western Cape, Modderdam Road, Bellville, Cape Town, South Africa
[3]Indian Institute of Geomagnetism, Navi Mumbai, India (satyavir@iigs.iigm.res.in)
[4]School of Physics, University of KwaZulu-Natal, Durban, South Africa

(Received 8 August 2011; revised 15 November 2011; accepted 16 November 2011; first published online 13 December 2011)

Abstract. The arbitrary amplitude Langmuir solitons are investigated in an unmagnetized, warm, relativistic plasma, consisting of electrons and positrons. Both the species are considered to have equal non-relativistic temperatures, but can have arbitrary relativistic drift speeds, and their dynamics are governed by fluid equations. Using the Sagdeev psuedo-potential approach, the effects of drift speed, Mach number, and thermal temperature on the amplitude and width of the Langmuir solitons are investigated. For the parameters considered, only rarefactive solitons are found. These solitons represent dip in electron density or electron holes in the configuration space. Existence domain of the Langmuir solitons is limited by the minimum and maximum Mach numbers for given parameters. An increase in the electron (positron) temperature leads to an increase in the Langmuir soliton amplitude and their half-widths. On the other hand, increasing the electron (positron) drift speeds results in decreasing soliton amplitudes and their half-widths. For some typical parameters corresponding to the pulsar magnetosphere, namely electron density $\sim 10^6$ cm^{-3} and electron thermal velocity of one-tenth of the velocity of light, the electric field of the Langmuir solitons can be of the order of (3–24) kV/m. The presence of such large amplitude electrostatic solitary structures may accelerate electrons and positrons and also produce fine structures of (1–5) microseconds in pulsar radio emissions.

1. Introduction

The study of relativistic effects in electron–positron (e–p) plasmas is of importance since it is known that these plasmas exist in pulsars (Beskin et al. 1983, Gurevich and Istomin 1985), active galactic nuclei (Henri et al. 1993, Hartman et al. 2001), and gamma ray bursts (Goodman 1986, Paczyński 1986, Eichler et al. 1989), where highly energetic charged particles are present. Yu et al. (1984) investigated the nonlinear propagation of intense circularly polarized electromagnetic waves in a magnetized electron–positron plasma, where the relativistic and ponderomotive force effects were included. Their analytical investigation determined that sharply spiked potential pulses existed in a strongly magnetized plasma, while a smooth pulse was present in a weakly magnetized, warm plasma and a moderately spiked pulse in a weakly magnetized, cold plasma. Large amplitude solitary Alfvén modes propagating at oblique angles in a magnetized cold relativistic electron–positron plasma have been studied by Verheest and Lakhina (1996). They employed the reductive-perturbation technique to derive the Kortweg-de Vries(KdV) equation and found that the nonlinearity vanishes for parallel propagation (to the ambient magnetic field), and is strongest at strictly perpendicular propagation. In a further study, Lakhina and Verheest (1997) included the pressure and ultra-relativistic effects. For parallel propagation, in the ultra-relativistic limit, linearly polarized subsonic Alfvén solitons were found to be possible, but supersonic Alfvén solitons did not exist. The Alfvén solitons for perpendicular propagation were found to have a different nature compared with those in cold relativistic plasmas (Verheest and Lakhina 1996).

Ion-acoustic waves in relativistic, three-component electron–positron-ion plasmas have been of recent interest. Gill et al. (2007) investigated ion-acoustic solitary waves in a weakly relativistic electron-positron-ion plasma using the reductive-perturbation technique to derive the KdV equation. Gill et al. (2007) studied the effect of plasma parameters such as temperature and density ratio of the electrons and positrons and the relativistic factor on the soliton structures. These parameters significantly affected the amplitude and width of the solitons. Moreover, the small amplitude study showed that only compressive solitons were possible. An increase in the relativistic effect resulted in an increase in the soliton amplitude. Abdelsalam et al. (2008) studied ion-acoustic solitary waves in electron-positron-ion

https://doi.org/10.1017/S0022377811000547 Published online by Cambridge University Press

plasmas using the Sagdeev pseudo-potential approach. They studied arbitrary amplitude soliton profiles as well as small amplitude profiles using the derived KdV equation. It was found that both subsonic and supersonic ion-acoustic solitary waves are possible for low values of the density ratio of positrons to electrons, but only subsonic solitons existed for high-density ratios.

On the other hand, in pure electron–positron plasmas, due to equal mass of electrons and positrons, the existence of ion acoustic-type modes is ruled out. However, it is possible to have the Langmuir modes in electron–positron plasmas. The reason for the existence of the linear and nonlinear Langmuir waves in electron–positron plasmas is that the density perturbations in the Poisson's equation do not cancel each other but add up due to opposite charges. This has been shown by Zank and Greaves (1995), where they studied small amplitude solitons with electrons and positrons having equal temperatures in non-relativistic plasmas.

The present study is an extension of the work by Bharuthram and Yu (1993), who investigated the existence and properties of finite amplitude electron plasma waves in an unmagnetized electron–ion plasma to the case of relativistic electron–positron plasma. At the same time, this paper generalizes the work by Zank and Greeves (1995) on the small amplitude Langmuir solitons in non-relativistic electron–positron plasmas to arbitrary amplitude solitons in relativistic electron–positron plasmas. We investigate the formation of Langmuir solitons in an unmagnetized, warm, relativistic plasma consisting of electrons and positrons through an arbitrary amplitude theory. Both species are considered to have a drift velocity and their dynamics are governed by fluid equations. Soliton profiles are examined as a function of plasma parameters such as the soliton speed, drift velocity, and relativistic factor. The organization of the paper is as follows: Arbitrary amplitude theory of the model is presented in Sec. 2, numerical results are presented in Sec. 3, and are summarized in Sec. 4.

2. Arbitrary amplitude theory

We consider a theoretical model consisting of relativistic electrons and positrons in unmagnetized plasmas with equilibrium densities, denoted by n_{e0} and n_{p0}, and equilibrium relativistic drift velocities, v_{e0} and v_{p0}, for electrons and positrons, respectively. However, the temperatures of both electrons, T_e, and positrons, T_p, are taken as non-relativistic. The dynamics of the model are governed by the following set of equations, namely, the continuity equation

$$\frac{\partial n_j}{\partial t} + \nabla \cdot (n_j \mathbf{v}_j) = 0, \tag{2.1}$$

and the momentum equation,

$$\frac{\partial \mathbf{P}_j}{\partial t} + (\mathbf{v}_j \cdot \nabla)\mathbf{P}_j = -\frac{T_j}{n_j}\nabla n_j - \alpha_j e \nabla \phi, \tag{2.2}$$

where the relativistic momentum $\mathbf{P}_j$ for the jth species is given by

$$\mathbf{P}_j = \frac{m_0 \mathbf{v}_j}{\left(1 - \frac{v_j^2}{c^2}\right)^{1/2}}, \tag{2.3}$$

where $j = e(p)$ for electrons (positrons) and $\alpha_j = -1(+1)$ for electrons (positrons). Here, n_j, T_j, and $\mathbf{v}_j$ are the densities, temperatures, and fluid velocities, respectively. The common rest mass of electrons and positrons is $m_0 = m_{e0} = m_{p0}$, c is the speed of light, and ϕ is the electrostatic potential.

The system is closed by the Poisson's equation,

$$\epsilon_0 \nabla^2 \phi = e(n_e - n_p). \tag{2.4}$$

Before proceeding to the arbitrary amplitude soliton theory, we would like to discuss the linear dispersion relation. The linear dispersion relation can be obtained from the above set of basic equations (2.1)–(2.4) by linearizing them and eliminating the first-order quantities. The general linear dispersion relation for such a plasma turns out to be

$$1 = \frac{\omega_{pe}^2 \sqrt{1 - \frac{v_{e0}^2}{c^2}}}{(\omega - k v_{e0})^2 - k^2 v_{te}^2} + \frac{\omega_{pp}^2 \sqrt{1 - \frac{v_{p0}^2}{c^2}}}{(\omega - k v_{p0})^2 - k^2 v_{tp}^2}, \tag{2.5}$$

where $\omega_{pj} = \sqrt{n_{j0} e^2 / \epsilon_0 m_0}$ is the plasma frequency of the jth species. For $T_e = T_p = T$, $n_{e0} = n_{p0}$ (quasi-neutrality condition) and $v_{e0} = v_{p0}$, the above dispersion relation can be reduced to

$$\omega = k v_0 \pm \sqrt{2\omega_{pe}^2/\gamma_0 + k^2 v_{te}^2}, \tag{2.6}$$

where $\gamma_0 = (1 - v_0^2/c^2)^{-1/2}$.

It must be emphasized here that due to equal masses of electrons and positrons, such plasmas cannot support acoustic modes but can support Langmuir waves, as is shown by dispersion relation (2.6). This is due to the fact that linear perturbations for electrons and positrons are equal but opposite and they add up in the Poisson's equation. For $k = 0$, no wave mode except plasma oscillations at $\omega_{pe}\sqrt{2/\gamma_0}$ exist. The Langmuir waves appear as wave number increases.

For the study of arbitrary amplitude solitons, (2.1)–(2.4) are transformed to a stationary frame moving with velocity V, the phase velocity of the wave, i.e. $\xi = x - Vt$, with wave propagation taken in the x direction. Hence, (2.1) can be integrated to yield

$$v_j = V\left(1 - \frac{n_0}{n_j}\right) + \frac{n_0 v_{j0}}{n_j}. \tag{2.7}$$

The plasma is assumed to be unperturbed at $\xi \to \pm\infty$, and satisfies the boundary conditions $n_{e0} = n_{p0} = n_0$ (n_0 being equilibrium electron (positron) density), $v_j = v_{j0}$, and $\phi = 0$ at $\xi \to \pm\infty$.

https://doi.org/10.1017/S0022377811000547 Published online by Cambridge University Press

Substituting (2.3) into (2.2) and integrating using the appropriate boundary conditions at $\xi \to \pm\infty$ yields for electrons,

$$\frac{e\phi}{m_0} = v_{th}^2 ln\left(\frac{n_e}{n_0}\right) + \frac{c^2}{\sqrt{1-\frac{v_e^2}{c^2}}} - \frac{c^2}{\sqrt{1-\frac{v_{e0}^2}{c^2}}} - \frac{v_e V}{\sqrt{1-\frac{v_e^2}{c^2}}} + \frac{v_{e0} V}{\sqrt{1-\frac{v_{e0}^2}{c^2}}}, \tag{2.8}$$

and for positrons,

$$-\frac{e\phi}{m_0} = v_{th}^2 ln\left(\frac{n_p}{n_0}\right) + \frac{c^2}{\sqrt{1-\frac{v_p^2}{c^2}}} - \frac{c^2}{\sqrt{1-\frac{v_{p0}^2}{c^2}}} - \frac{v_p V}{\sqrt{1-\frac{v_p^2}{c^2}}} + \frac{v_{p0} V}{\sqrt{1-\frac{v_{p0}^2}{c^2}}}, \tag{2.9}$$

where $v_{th} = \sqrt{T/m_0}$ is the thermal speed of electrons and positrons. The Poisson's equation in transformed coordinates can be written as

$$\frac{d^2\phi}{d\xi^2} = \frac{e}{\epsilon_0}(n_e - n_p). \tag{2.10}$$

Using (2.7) in (2.8)–(2.10), the normalized form of (2.8) and (2.9) is given by

$$\phi_e = \Phi = lnN_e + \frac{C^2\left[N_e - M^2\left(N_e - 1 + \frac{V_{e0}}{M}\right)\right]}{\sqrt{N_e^2 - M^2\left(N_e - 1 + \frac{V_{e0}}{M}\right)^2}} - \frac{C^2(1 - MV_{e0})}{\sqrt{1 - V_{e0}^2}} \tag{2.11}$$

and

$$\phi_p = -\Phi = lnN_p + \frac{C^2\left[N_p - M^2\left(N_p - 1 + \frac{V_{p0}}{M}\right)\right]}{\sqrt{N_p^2 - M^2\left(N_p - 1 + \frac{V_{p0}}{M}\right)^2}} - \frac{(C^2 - MV_{p0})}{\sqrt{1 - V_{p0}^2}}, \tag{2.12}$$

and the normalized form of the Poisson's equation (2.10) becomes

$$\frac{d^2\phi_e}{d\zeta^2} = N_e - N_p, \tag{2.13}$$

where $N_e = n_e/n_0$ and $N_p = n_p/n_0$ are the normalized electrons and positron densities, respectively, $M = V/c$ is the Mach number, $V_{j0} = v_{j0}/c, C = c/v_{th}$, $\Phi = \frac{e\phi}{T}$, distance ξ is normalized by the electron (positron) Debye length $\lambda_d = \sqrt{\epsilon_0 T/n_0 e^2}$, and time t is normalized with respect to inverse of plasma frequency, i.e. $\omega_p^{-1} = \sqrt{\epsilon_0 m_0/n_0 e^2}$. Addition of (2.11) and (2.12) yields the following equation,

$$lnN_e + \frac{C^2\left[N_e - M^2\left(N_e - 1 + \frac{V_{e0}}{M}\right)\right]}{\sqrt{N_e^2 - M^2\left(N_e - 1 + \frac{V_{e0}}{M}\right)^2}} - \frac{C^2(1 - MV_{e0})}{\sqrt{1 - V_{e0}^2}} = -lnN_p - \frac{C^2\left[N_p - M^2\left(N_p - 1 + \frac{V_{p0}}{M}\right)\right]}{\sqrt{N_p^2 - M^2\left(N_p - 1 + \frac{V_{p0}}{M}\right)^2}} + \frac{(C^2 - MV_{p0})}{\sqrt{1 - V_{p0}^2}} \tag{2.14}$$

Integrating (2.13) once w.r.t. ζ and using (2.11) and (2.12), we obtain the following energy integral,

$$\frac{1}{2}\left(\frac{dN_e}{d\zeta}\right)^2 + \psi(N_e, N_p, M) = 0, \tag{2.15}$$

where the normalized form of the Sagdeev potential represented in terms of densities is given by

$$\psi(N_e, N_p, M) = \frac{\psi_1 + \psi_2}{\left[\frac{1}{N_e} - \frac{C^2M^2\left(1 - \frac{V_{e0}}{M}\right)^2}{\left(N_e^2 - M^2\left(N_e - 1 + \frac{V_{e0}}{M}\right)^2\right)^{3/2}}\right]^2}, \tag{2.16}$$

where

$$\psi_1 = 1 - N_e - C^2M^2\left[\frac{\frac{V_{e0}}{M}\left(1 - \frac{V_{e0}}{M}\right)}{\sqrt{1 - V_{e0}^2}} - \frac{\left(1 - \frac{V_{e0}}{M}\right)\left(N_e - 1 + \frac{V_{e0}}{M}\right)}{\left[N_e^2 - M^2\left(N_e - 1 + \frac{V_{e0}}{M}\right)^2\right]^{1/2}}\right] \tag{2.17}$$

and

$$\psi_2 = 1 - N_p - C^2M^2\left[\frac{\frac{V_{p0}}{M}\left(1 - \frac{V_{p0}}{M}\right)}{\sqrt{1 - V_{p0}^2}} - \frac{\left(1 - \frac{V_{p0}}{M}\right)\left(N_p - 1 + \frac{V_{p0}}{M}\right)}{\left[N_p^2 - M^2\left(N_p - 1 + \frac{V_{p0}}{M}\right)^2\right]^{1/2}}\right]. \tag{2.18}$$

To obtain soliton solutions from (2.15), the Sagdeev potential $\psi(N_e, N_p, M)$ must satisfy the conditions: $\psi(N_e, N_p, M) = 0$, $d\psi(N_e, N_p, M)/dN_e = 0$, $d^2\psi(N_e, N_p, M)/dN_e^2 < 0$ at $N_e = 1 = N_p$; $\psi(N_e, N_p, M) = 0$ at some value of $N_e = N_0$ and $\psi(N_e, N_p, M) < 0$ for $N_0 < N_e < 1$. When the above-stated conditions are satisfied, the pseudo-particle is reflected in the pseudo-potential well at $N_e = N_0$ and returns to its initial state for solitary wave structures.

3. Numerical results

Numerical computations of (2.15) and (2.16) are done to evaluate the density profiles and Sagdeev potential, respectively, for solitary structures in electron–positron plasmas. For simplicity, the Sagdeev potential has been expressed in terms of electron density rather than the real potential. It may be noted that though the first term

https://doi.org/10.1017/S0022377811000547 Published online by Cambridge University Press

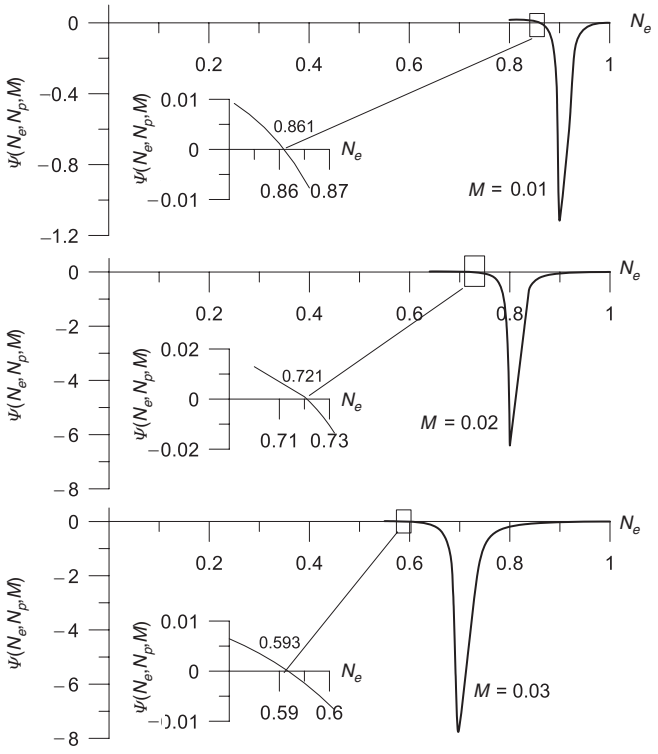


Figure 1. The Sagdeev potential $\psi(N_e, N_p, M)$ vs. N_e for different Mach numbers, M = 0.01(top panel), 0.02 (middle panel), and 0.03 (bottom panel) as shown in the curves. The fixed parameters are $v_{e0}/c = v_{p0}/c = 0.1$ and $c/v_{th} = 10.0$. The small figures show the blown-up portions of the rectangles in each panel to clearly show the crossing of N_e axis.

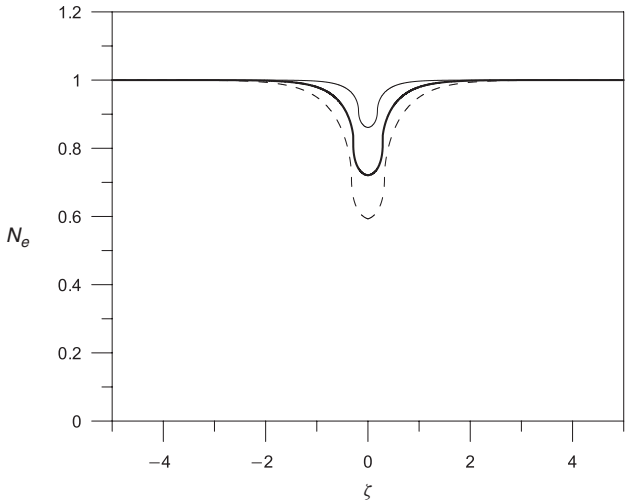


Figure 2. Soliton profiles for the corresponding parameters of Fig. 1. for M = 0.01 (solid), 0.02 (dotted), 0.03 (broken).

in the energy integral (2.15) is written in terms of electron density, the Sagdeev potential, $\psi(N_e, N_p, M)$, also contains terms corresponding to the positron density. The positron density, N_p is calculated using (2.14) for a given electron density, N_e. Subsequently, the calculated positron density, N_p is used to evaluate the Sagdeev potential, $\psi(N_e, N_p, M)$, given by (2.16) and the soliton amplitude profile using (2.15) by employing the Runge–Kutta method for numerical integration.

The Sagdeev potential, $\psi(N_e, N_p, M)$, is always zero at $N_e = 1 = N_p$ and for given values of V_{e0} and V_{p0} which can be verified analytically from (2.16)–(2.18). Further, the first derivative of the Sagdeev potential at $N_e = 1 = N_p$ also vanishes due to quasi-neutrality in the equilibrium state. The condition $d^2\psi(N_e, N_p, M)/dN_e^2 < 0$ at $N_e = 1 = N_p$ is satisfied provided the Mach number exceeds a minimum value, $M_{\min}$. It is complicated to get an analytical expression for $M_{\min}$ for the Sagdeev potential given by (2.16). It is important to note from the Sagdeev potential $\psi(N_e, N_p, M)$ given by (2.16) that the conditions $N_e^2 - M^2(N_e - 1 + \frac{V_{e0}}{M})^2 > 0$ and $N_p^2 - M^2(N_p - 1 + \frac{V_{p0}}{M})^2 > 0$ have to be satisfied to have a meaningful solution. These conditions provide an upper limit of the Mach number, $M_{\max} = (V_{0j} + N_j)/(1 - N_j)$, where $j = e, p$, beyond which solitary solutions do not exist.

The numerical results are presented in the form of graphs. Figure 1 shows the typical form of the Sagdeev potential $\psi(N_e, N_p, M)$ versus N_e for Mach numbers, $M(= V/c) = 0.01$ (top panel), 0.02 (middle panel), and 0.03 (bottom panel) as shown on the curves. The other fixed parameters are normalized electron drift speed $V_{e0}(= v_{e0}/c) = 0.1$, normalized positron drift speed $V_{po}(= v_{p0}/c) = 0.1$, and $C(= c/v_{th}) = 10.0$. The Sagdeev potential, $\psi(N_e, N_p, M)$, plotted in Fig. 1 is peculiar, it attains large values but is continuous. The solution for (2.15) consists of a localized density depressions, i.e. $N_e \ll 1$.

For clarity, in each panel of Fig. 1, we have plotted smaller figures to show exactly where the Sagdeev potential curves cross the N_e axis other than at $N_e = 1$ value. The small figures show the blown-up portions of the rectangles in each panel. For M = 0.01, 0.02, and 0.03, the curves cross N_e axis at N_e= 0.861, 0.721, and 0.593, respectively, as shown in small figures.

The corresponding soliton profiles obtained by numerical integration of (2.15) are plotted in Fig. 2. As the soliton speed or the Mach number M increases, it is found that the amplitude of the soliton (i.e. the depth of the density profile) also increases. These are rarefactive solitons or electron holes. These are bulb types of solitons and have been studied earlier by several workers (Porkolab and Goldman 1976, Yu 1978, Bharuthram and Yu 1993, Wei and Chen 2005, Ghosh et al. 2008).

Figure 3 shows the variation of soliton amplitude for various values of $c/v_{th} = 10.0$ (solid), 13 (dotted), and 15 (broken) with Mach number, $M = 0.05$ and $V_{e0} = V_{p0} = 0.1$. It can be seen from the curves that as c/v_{th} increases, i.e. temperature of electrons or positrons decreases, the soltion amplitude decreases. The solitons become narrower with a corresponding decrease in the half-width and have a bulb-type shape. The effect of equal drift speeds of two species (electrons and positrons) streaming in the same direction is studied in Fig. 4. The drift speeds are varied from $V_{e0} = V_{p0} = 0.10$ (solid),

https://doi.org/10.1017/S0022377811000547 Published online by Cambridge University Press

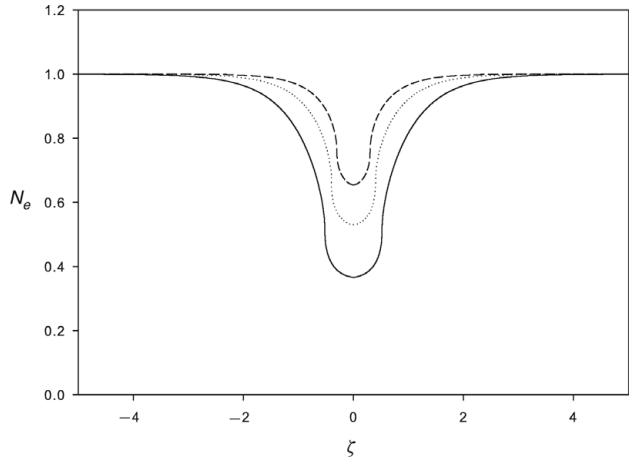


Figure 3. Soliton profiles for $c/v_{th} = 10.0$ (solid), 13 (dotted), 15 (broken) for the parameters, Mach number, $M = 0.05$, and $v_{e0}/c = 0.1 = v_{p0}/c$.

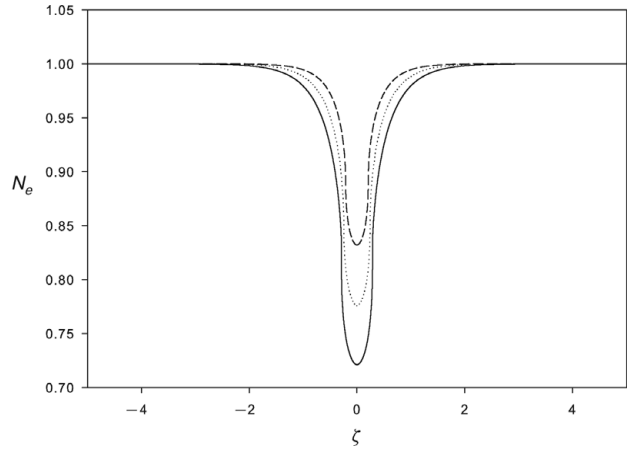


Figure 4. Soliton profiles for equal electron and positron drift speeds $v_{e0}/c = v_{p0}/c = 0.10$ (solid), 0.105 (dotted), 0.11 (broken). The fixed parameters are $M = 0.02$ and $c/v_{th} = 10.0$.

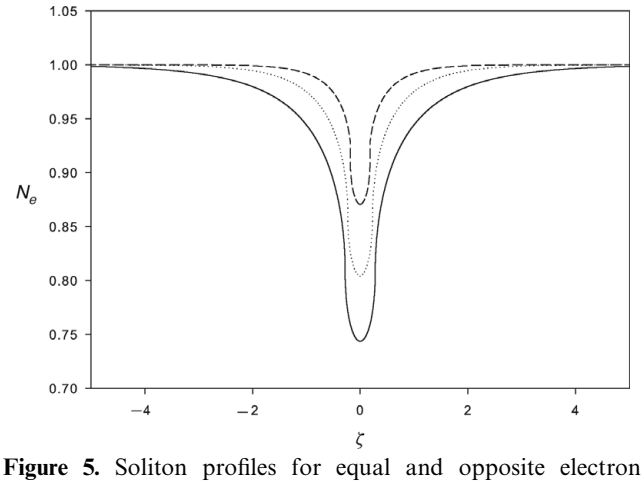


Figure 5. Soliton profiles for equal and opposite electron and positron drift speeds $v_{e0}/c = 0.10$, $v_{p0}/c = -0.10$ (solid), $v_{e0}/c = 0.105$, $v_{p0}/c = -0.105$ (dotted), $v_{e0}/c = 0.11$, $v_{p0}/c = -0.11$ (broken). The fixed parameters are $M = 0.02$ and $c/v_{th} = 10.0$.

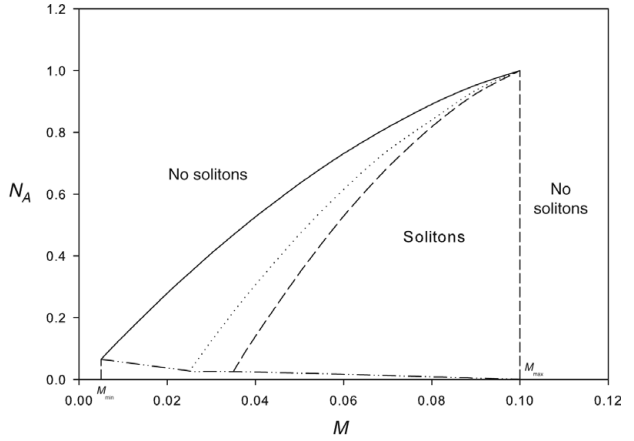


Figure 6. The maximum soliton amplitude N_A as a function of the Mach number for $c/v_{th} = 10.0$ (solid), 13 (dotted) and 15 (broken) with $v_{e0}/c = v_{p0}/c = 0.1$.

0.105 (dotted), 0.11 (broken), and other fixed parameters are $M = 0.02$ and $c/v_{th} = 10.0$. An increase in the drift speed results in a decrease in the soliton amplitude. The soliton profiles for the case of equal speeds but counter-streaming electrons and positrons are shown in Fig. 5. It is noted that soliton amplitudes are slightly smaller, but there is a similar trend when compared with electrons and positrons having equal drifts and streaming in the same direction (Fig. 4). The soliton profiles in Figs. 4 and 5 are much sharper and narrower than in Figs. 2 and 3.

Figure 6 shows the existence domain of solitons in the relativistic electron–positron plasmas for typical set of parameters. The figure shows the maximum soliton amplitude (N_A) as a function of Mach number, M. The figure was constructed in the following manner. For each value of c/v_{th}, the range of M values for which solitons were possible were established. The parameters used in plotting the soliton amplitude versus M are as follows: $c/v_{th} = 10.0$ (solid), 13 (dotted), and 15 (broken) with $v_{e0}/c = v_{p0}/c = 0.1$. For a fixed value of c/v_{th}, no solutions exist to the left ($M_{\min}$) and the right ($M_{\max}$) of the endpoint M-values of a particular curve. It is interesting to note that the numerical value of $M_{\max}$ matches with the analytical expression for $M_{\max} = V_0$ when $N_j \to 0$. This explains the convergence of all curves to the value 0.1 as M increases. It is seen from the figure that as c/v_{th} increases, the range of M values for which soliton structures to exist decreases. In addition, $M_{\min}$ increases with c/v_{th}.

4. Summary

The existence of arbitrary amplitude solitons in a relativistic electron–positron, unmagnetized plasmas has been investigated. The model consists of electrons and positrons having equal temperatures (non-relativistic), but any arbitrary equilibrium drift speeds. The Sagdeev pseudo-potential approach is used to derive the energy-integral for arbitrary amplitude solitons. It is shown that the electrostatic fluctuations can propagate as nonlinear

https://doi.org/10.1017/S0022377811000547 Published online by Cambridge University Press

rarefactive *Langmuir* solitons. Therefore, these structures form density cavities or electron holes in the configurational space. For typical range of parameters, our model shows that an increase in the soliton speed results in an increase in soliton amplitude. For warmer electron–positron plasmas ((c/v_{th}) decreasing) the results show that the soliton amplitude would increase. Increasing c/v_{th} also results in decrease in the soliton half-widths. The effect of electrons and positrons having equal drift speeds and streaming in the same direction on the soliton amplitude is similar to electrons and positrons having equal drift speeds in opposite directions. However, in the latter case the soliton amplitudes are somewhat smaller. The existence domain of soliton structures is found to be limited by the minimum and maximum Mach numbers for the chosen plasma parameters.

Our result may be useful in understanding nonlinear phenomena in astrophysical plasmas as well as laboratory experiments where relativistic electrons and positrons are observed. As an example, we consider the case of pulsar magnetosphere. The electron–positron densities vary over several order of magnitude depending upon the position of the source region from pulsar surface. Let us consider the equilibrium electron or positron density as $n_0 = 10^6\,\mathrm{cm}^{-3}$, which is a representative value at about 100 pulsar radii (Melrose 1978). Then, for the parameters considered here, namely, $C = c/v_{th}$=10, $M = V/c = 0.01$–0.05, and electron or positron drifts $v_{e0}/c = v_{p0}/c$= 0.1, we have typical normalized soliton density dips $N_e \approx (0.1$–$0.5)$, with soliton widths, $W =$ 4–5 (see Figs. 2–5). This would give soliton electric field of the order of $E = (T/e\lambda_d).(N_e W) \approx (4\text{-}24) \times 10^3\,\mathrm{V/m}$. The electric fields of the solitary structures would be bipolar in nature. Such large electric fields may give rise to significant acceleration of electrons and positrons. Furthermore, the presence of large amplitude electrostatic solitary structures may modulate the energetic electrons (positrons) producing pulsar radio emission. This modulation will have typical time scale of $\tau =$ soliton width/soliton speed $= (1$–$5) \times 10^{-6}$ s. As a result of this, the pulsar radiations will have fine structures of $\sim(1$–$5)$ microseconds.

In our model, we have included relativistic effects in the velocity but not in the temperature. Thus, validity of our model is for small and non-relativistic temperature. However, one can include relativistic temperature in order to see its effect. This is beyond the scope of the present analysis.

Acknowledgements

SVS acknowledges the support and hospitality provided at Physics Department, University of the Western Cape, Bellville, South Africa. GSL thanks Indian National Science Academy, New Delhi for support under the Senior Scientist Scheme.

References

Abdelsalm, U. M., Moslem, W. M. and Shukla, P. K. 2008 *Phys. Lett*. A **372**, 4057.

Beskin, V. S., Gurevich, A. V. and Istomin, Ya. N. 1983 *Soviet Phys. JETP* **58**, 235.

Bharuthram, R. and Yu, M. Y. 1993 *Astrophys. Space Sci.* **207**, 197.

Eichler, D., Livio, M., Piran, T. and Schramm, D. N. 1989 *Nature* **340**, 126.

Ghosh, S. S., Pickett, J. S., Lakhina, G. S., Winningham, J. D., Lavraud, B. and Decreau, P. M. E. 2008 *J. Geophys. Res.* **113**, A06218, doi:10.1029/2007JA012768

Gill, T. S., Singh, A., Kaur, H., Saini, N. S. and Bala, P. 2007 *Phys. Lett*. A **361**, 364.

Goodman, J. 1986 *Astrophys. J.* **308**, L47.

Gurevich, A. V. and Istomin, Ya. N. 1985 *Soviet Phys. JETP* **62**, 1.

Hartman, R. C., Villata, M., Balonek, T. J., Bertsch, D. L., Bock, H., Böttcher, M., Carini, M. T., Collmar, W., De Francesco, G., Ferrara, E. C., et al. 2001 *Astrophys. J.* **558**, 583.

Henri, G., Pelletier G. and Roland, J. 1993 *Astrophys. J.* **404**, L41.

Lakhina, G. S. and Verheest, F. 1997 *Astrophys. Space Sci.* **253**, 97.

Melrose, D. B. 1978 *Astrophys. J.* **225**, 557.

Paczyński, B. 1986 *Astrophys. J.* **308**, L43.

Porkolab, M. and Goldman, M. V. 1976 *Phys. Fluids* **19**, 872.

Verheest, F. and Lakhina, G. S. 1996 *Astrophys. Space Sci.* **240**, 215.

Wei, R. and Chen, Y. 2005 *Physica Scripta* **71**, 648.

Yu, M. Y. 1978 *J. Math. Phys.* **19**, 816.

Yu, M. Y., Shukla, P. K. and Rao, N. N. 1984 *Astrophys. Space Sci.* **107**, 327.

Zank, G. P. and Greaves, R. G. 1995 *Phys. Review* E, **51**, 6079.

https://doi.org/10.1017/S0022377811000547 Published online by Cambridge University Press